Exponential Sum Modeling of Reswick and Rogers Pressure-Duration Curve: A New Analysis and Model

Oscar A. Linares[1,*], Darko Stefanovski[2] and Raymond C. Boston[3]

[1]*Wayne State University, Detroit, MI 48202, USA and Pharmacokinomics & Exotic Modeling Unit, 751 S. Military Rd., Dearborn, MI 48124, USA*

[2]*Cedars-Sinai Medical Center, Biomedical Sciences Division, 8700 Beverly Boulevard West Hollywood, CA 90048, USA*

[3]*Department of Biostatistics and Epidemiology, University of Pennsylvania, New Bolton Center, 382 West Street Road, Kennett Square, PA 19348, USA*

Abstract: Reswick and Rogers model is not valid for predicting the effects of short- and long-time tissue exposures to contact pressures because it lacks intercepts. A different model, without those asymptotic properties, that could fit the shape of the curve well, could potentially provide useful information. We used modeling to test the hypotheses that an exponential model could fit Reswick and Rogers pressure-duration curve, and, if so, to determine the order of the best fit exponential model. Up to four exponential sum models were fit. Three exponentials provided the best fit [Weighted sum-of-squared residuals 72, Akaike Information Criterion 89, r=0.997]. Thereby identifying three homogeneously distinct anatomical pressure-load containing tissue compartments: skin, fat, and muscle. A fourth compartment, bone, could not be identified because of limited resolution of the data. Our results suggest that the fat pressure-load containing compartment may play an adaptive compensatory preventive role in response to pressure loads—"a cushion effect." Exponential sum modeling of pressure-duration curves provides a new approach for studying the dynamics of compression in normal and disease states in humans, and it may be useful for practical application at the point-of-care to assist with prevention and treatment of pressure ulcers.

Keywords: Nonlinear regression, curve fitting, parameter estimation, modeling, pressure sores, pressure ulcers, wounds, pressure-duration curve, SAAM, WinSAAM.

INTRODUCTION

Exponential sum models are commonly used to investigate systems of biological interest in biochemistry [1], ecology [2], physiology [3], and pharmacology [4-6], and they play an important role in developing an understanding of real human systems [7]. These models have served as mathematical probes for sampling inaccessible regions of the body [3, 8-10], so they may be useful for quantifying biomechanical responses of human tissues to externally applied pressure loads *in vivo*.

Mathematical modeling is becoming increasingly popular for the description of biomechanical processes. Recently, six mathematical functions used in biomechanical modeling to investigate cell and tissue damage have been studied [11]. Surprisingly, however, exponential sum models were not included. This is probably because exponential sum models have not been used to investigate deep tissue injury in biomechanical engineering [12]. But, in the closely related area of wound management, the area of skin a pressure sore covers over time decreases exponentially [13, 14]. Therefore, this approach might provide new insight into the dynamics of the Reswick and Rogers [15] pressure-duration curve in humans.

Reswick and Rogers [15] linked level of skin-to-surface interface pressure, or contact pressure [P_C mmHg], to P_C duration [t hr]. They found a hyperbolic relationship between P_C and duration [15]. Because a hyperbola does not have a y- or x-intercept, Gefen [8, 16] concluded that the Reswick and Rogers model is not valid for predicting the effects of short- and long-time tissue exposures to P_C. However, Gefen [16], identified a predictive domain of validity for the Reswick and Rogers model. This indicates that the problem with the Reswick and Rogers model is its asymptotic properties. A different model, without the asymptotic properties of their model, that could fit the shape of their pressure-duration curve well, could potentially provide useful information.

Therefore, modeling was performed to determine whether the Reswick and Rogers [15] pressure-duration curve could be fit using a sum of exponentials model, and, if so, to determine the order of the best fit exponential model.

*Address corresponding to this author at the PRS Wound Management, P.C., 20927 Kelley Road, Eastpointe, MI 48021, USA; Tel: (734) 735-4022; Fax: (734) 453-7019; E-mail: oscar.linares@wayne.edu

ISSN: 1814-8085 / E-ISSN: 1927-5129/12

METHODS

Data

The data for exponential model identification was extracted from the published Reswick and Rogers [15] pressure-duration curve using established methodology [17, 18]. Digital reconstruction of their pressure-duration curve for numerical identification was performed as previously described by Boston and Moate [19, 20]. Subject demographics and experimental protocols have been fully described in Reswick and Rogers [15].

Modeling

The Reswick and Rogers [15] pressure-duration curve data was of type,

$$y(t) = f\left(t;\mathbf{p}\right), \tag{1}$$

where t is time and $\mathbf{p}$ is a P-dimensional vector containing the set of $\mathbf{p}$ parameters in f to be estimated. The exponential sum models chosen for fitting were:

$$y_i(t) = \sum_{i=1}^{4} A_i e^{-\alpha_i t},\ A \geq 0,\ \ \alpha_i \geq 0. \tag{2}$$

The measurement error was assumed to be additive, independent, Gaussian, with a mean of zero, and a standard deviation determined from the data.

Modeling was performed using WinSAAM [21]. A nonlinear weighted-least squares estimation method was used to estimate the unknown parameter vector

$$\mathbf{p} = \left[A_1,\ A_2,...,A_4,\ \alpha_1,\ \alpha_2,...,\alpha_4\right]^T. \tag{3}$$

The weighted sum-of-squared residuals [WRSS] objective function is:

$$\mathrm{WRSS}\left(\mathbf{p}\right) = \sum_{i=1}^{N} w_i \left[\frac{y\left(t_i\right) - y\left(t_i,\mathbf{p}\right)}{SD\left(t_i\right)}\right]^2 \tag{4}$$

where N is the number of observations, $[\,y\left(t_i\right) - y\left(t_i,\mathbf{p}\right)]$ is the error between the observed and predicted value, respectively, for each P_C sample time t_i, $SD[t_i]$ is the standard deviation of the measurement error, and w_i is the weight assigned to the i^{th} datum.

The exponential model fits were evaluated on the basis of visualization, r values, the WRSS[**p**] and the accuracy of the parameter estimates [22, 23]. The Cramèr-Rao asymptotic lower bound of the covariance matrix was computed from the inverse of the Fisher information matrix:

$$\mathrm{Cov}[\mathbf{p}] \geq \left\{\left.\frac{\partial f}{\partial \mathbf{p}}\right|_{\mathbf{p}=\mathbf{p}} \mathrm{Cov}[y] \left.\frac{\partial f}{\partial \mathbf{p}}\right|_{\mathbf{p}=\mathbf{p}}\right\}^{-1}. \tag{5}$$

The derivatives were computed analytically from Equation 2 and evaluated at the parameter estimates $\mathbf{p}$. The standard deviations of $\mathbf{p}$ were obtained as the square roots of the diagonal elements of Cov[$\mathbf{p}$]. The estimability of the parameters was assessed using the coefficient of variation [CV]:

$$\mathrm{CV}(\mathbf{p}) = \frac{\sqrt{\mathrm{diag}\left(\mathrm{Cov}[\mathbf{p}]\right)}}{\mathbf{p}} \times 100. \tag{6}$$

A parameter was considered *a posteriori identifiable* [16] if its CV< 50%. This is because the 95% confidence interval of an estimate,

$$\mathbf{p} \pm \mathrm{t}\sqrt{\mathrm{diag}\left(\mathrm{Cov}[\mathbf{p}]\right)}, \tag{7}$$

where t is the value of the t-distribution with [N, dim[**p**]] degrees of freedom, includes zero if $\sqrt{\mathrm{diag}\left(\mathrm{Cov}[\mathbf{p}]\right)} \geq \mathbf{p}/2$ [7].

The selection of the best exponential model was made on the basis of the Akaike Information Criterion [AIC], which accounts for both goodness of fit and model parameter number [22]:

$$\mathrm{AIC} = N\ \ln(\mathrm{WRSS}) + 2P, \tag{8}$$

where WRSS represents the weighted sum-of squared residuals at $\mathbf{p}$, N is the number of data points and P is the number of exponential model parameters. The nonlinear regression correlation coefficient was defined as,

$$r = \sqrt{1 - \frac{SSE}{SST}}, \tag{9}$$

where SSE is the sum of squared standard errors and SST is the total sum-of-squared residuals.

Model Pressure-Load Indices

Three exponentials gave the best fit [see Results]. This means that P_C is transmitted through at least three homogeneously distinct anatomical pressure-load containing tissue compartments [24]: skin, fat, and

muscle [tissue compartment i = 1, 2, 3, respectively]. The areas under the curve [AUC_i] of each exponential component quantify the extent of pressure-load on each tissue compartment i:

$$\int_0^\infty y_i(t)\,dt = AUC_i = \frac{A_1}{\alpha_1} + \cdots + \frac{A_i}{\alpha_i},\ i = 1,\ 2,\ 3. \qquad (10)$$

The area under the first moment curve is

$$\int_0^\infty ty(t)\,dt = \mathrm{AUMC}_i = \frac{A_1}{[\alpha_1]^2} + \cdots + \frac{A_i}{[\alpha_i]^2},\ i = 1,\ 2,\ 3. \qquad (11)$$

From Equations 10 and 11, the mean tissue pressure-load time [MTPLT] is

$$\mathrm{MTPLT}_i = \frac{\mathrm{AUMC}_i}{\mathrm{AUC}_i},\ i = 1,\ 2,\ 3\ , \qquad (12)$$

where MTPLT_i is the average time that tissue i can sustain a pressure-load of P_{av} = $\mathrm{AUC}_i/\mathrm{MTPLT}_i$ before damage ensues. P_{av} is the average tissue pressure-load on tissue compartment i. From the exponential function, $T\alpha_i$ equals $2.303/\alpha_i$ represents the time that tissue i can sustain a maximum pressure-load of P_{max} [P_{max} = $\mathrm{AUC}/T\alpha_i$] before damage ensues. The pressure half-time [$PT_{1/2}$] is the time that tissue i can sustain a pressure-load equal to 50% of P_{av} before damage ensues. From the exponential function, $PT_{1/2}=0.693/\alpha_i$.

RESULTS

The one-exponential model did not fit the data well (Figure **1**). It fit the shoulder of the curve [$0 \le t < 2$ hr], but did not fit the elbow [$2 \le t \le 6$ hr] or arm [t > 6 hr] of the curve. The two-exponential model did not fit the data well either (Figure **1**); it fit the shoulder and elbow of the curve, but it did not fit the arm of the curve. Regardless, the fits produced r values > 0.98 (Table **1**). Moreover, the parameter estimates of both the one- and two-exponential models gave physically realizable values, and were accurately estimated (Table **1**).

In contrast, the tri-exponential model fit the shoulder, elbow, and arm of the curve well (Figure **1**). Four exponentials gave no significant improvement in the fit over that obtained with three exponentials. The tri-exponential model fit was better than the fits of both the one- and two-exponential models in terms of visualization, weighted sum-of-squared residuals, and most important, the Akaike Information Criterion (Table **1**). All of the tri-exponential model parameters were also accurately estimated.

The estimated total three-layer tissue pressure-load was equal to A_1 [skin] + A_2 [fat] + A_3 [muscle] = 1184 mmHg (Table **1**). The inset in Figure **1** displays a semi-log plot of the three distinct linearly decreasing tissue pressure-loads identified by the tri-exponential model, and their homogeneously distinct anatomical

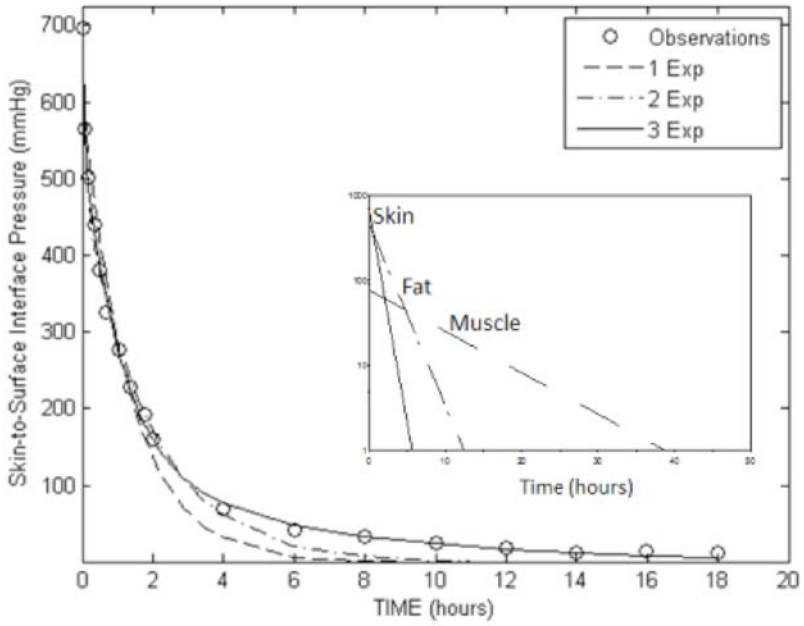

Figure 1: Observed contact pressures fell rapidly over time. Neither a single- or double-exponential model fit the data well. Note that the best fit of the observations occurred with three exponentials. The three exponential model identified three homogeneously distinct linearly decreasing tissue pressure-load distributions corresponding anatomically with skin, fat, and muscle (semilog inset plot).

Table 1: One, two, and three exponential models best fit parameter estimates, and their corresponding number of observations for fitting (*N*), weighted sum-of-squared residuals of best fit (WRSS), nonlinear correlation coefficient (*r*), parameter number (*P*), and Akaike Information Criterion (AIC)*

Parameters	1 Exponential	2 Exponentials	3 Exponentials
A_1	603 (0.5)	500 (5)	650 (1)
α_1	0.7398 (1)	0.7702 (9)	1.1469 (3)
A_2		68 (16)	457 (5)
α_2		0.1033 (12)	0.4905 (7)
A_3			77 (6)
α_3			0.1117 (5)
N	18	18	18
WRSS	23427.00	110.57	72.33
r	0.999	0.989	0.997
P	2	4	6
AIC	185	92.70	89.06

*Values in parentheses are coefficient of variation (CV) of parameter estimates in percent, calculated as $\mathrm{CV}(\mathbf{p})=\frac{\sqrt{\mathrm{diag}\left(\mathrm{Cov}[\mathbf{p}]\right)}}{\mathbf{p}}\times 100$. A parameter is considered *a posteriori identifiable* if its CV< 50%.

correlates. The plot shows that P_C is rapidly transmitted through skin, to fat, but, that it is transmitted through fat, to muscle, much more slowly. The transmission of P_C was dampened by the tissues as reflected by the fall in both P_{av} and P_{max} for each tissue *i* (Table **2**). Fat tissue dampened the P_C by about 83%.

The AUC indicated that the extent of pressure-load on fat was greater than that for both skin and muscle, but that it was greater for muscle compared to skin (Table **2**). Because of the dampening effect of P_C transmission through the tissues, the tissue MTPLT, $T\alpha_i$, and $PT_{1/2}$ were muscle > fat > skin (Table **2**).

DISCUSSION

The present study demonstrates that a sum of three exponentials model is the minimal model that provides a good description of the Reswick and Rogers [15] pressure-duration curve. We also numerically identified the specific sum of exponentials model with the minimum number of parameters and assumptions, but which still is consistent with the data used to construct it. This minimal exponentials model revealed that the P_C is transmitted through at least three homogeneously distinct pressure-containing compartments: skin, fat, and muscle; indicating that P_C results from the interactions of the homogeneous distribution and redistribution of tissue pressure loads, and their partitioning into more than one anatomical region. Thus tissue pressure loads can be modulated through a change in one or more of these determinants.

Numerical identifiability of parameter estimates, i.e., uniqueness of solutions, in our study were assessed using coefficients of variation. Our results indicate that

Table 2: Values of Minimal Triexponential Model Tissue Pressure-Load and Time Indices

TISSUE *i*	AUC mmHg × hr	AUMC mmHg × hr^2	MTPLT hr	P_{av} mmHg	$T\alpha_i$ hr	P_{max} mmHg	$PT_{1/2}$ hr
Skin	566	494	0.87	650	2.01	282	0.60
Fat	932	1903	2.04	457	4.70	198	1.41
Muscle	686	6081	8.87	77	20.61	33	6.20

AUC is area under the curve of tissue *i* (Text Eq. 10); AUMC is area under the first moment curve of tissue *i* (Text Eq. 11); MTPLT is the mean tissue pressure-load time for tissue *i*. It represents the average time that tissue *i* can sustain a pressure-load of P_{av} = AUC$_i$/MTPLT$_i$ before damage ensues; P_{av} is the average tissue pressure-load on tissue *i*; $T\alpha_i$ equals 2.303/α_i is the time that tissue *i* can sustain a maximum pressure-load of P_{max} (P_{max} = AUC/$T\alpha_i$) before damage ensues; The pressure half-time ($PT_{1/2}$) is the time that tissue *i* can sustain a pressure-load equal to 50% of P_{av} before damage ensues: $PT_{1/2}$=0.693/α_i.

our model parameters were both uniquely numerically identifiable and estimable. Exponential functions are mechanistic as opposed to statistical model functions that could also have fitted the data well. Neither a high-order polynomial function nor a statistical model could have identified the compartmental tissue compartments identified in this study.

A goal in this study was to begin to address the heterogeneity of distribution of pressure duration for use in bedside clinical diagnosis in the course of treatment of pressure wounds. Our goal was not to provide a detailed biomechanical account of the three dimensional stress states that tissues are exposed too, not to study the influence that bony prominences would have on creating focal tissue deformations and stresses, particularly at bone-muscle contact regions. These are irrelevant at the bedside.

Sopher and coworkers [25] found that they could modulate internal tissue loads by varying fat and muscle tissue mass determinants. In our model, varying fat and muscle tissue determinants means manipulating the eigenvectors and eigenvalues of our model, the A_i and α_i, which correspond to tissue pressure loads and their transmission rates, respectively. Using finite element modeling [26], tissue pressure load is heterogeneously distributed between skin, fat, and muscle tissue. The upper 95% confidence interval for total tissue pressure load is 1146 mmHg, a value which differs from our models prediction of 1184 mmHg by only 3%.

The standard value for capillary closing pressure is 32 mmHg [27]. This value has been confirmed by McLennan and coworkers [28] and numerous other studies [29, 30], although a value of 29 mmHg has been reported for women [31]. We found that P_{max} for muscle tissue was equal to 33 mmHg. This value coincides with estimated critical capillary closing pressures. Moreover, our model predicts that muscle tissue can only sustain such a pressure for about 21 hours, which is consistent with the notion that both level and duration of pressure-load are important determinants of muscle injury.

Our model overcomes the asymptotic limitations of the Reswick and Rogers model [15] identified by Gefen [32] because our model does not predict infinitely large P_C values for short-time pressure load exposures, nor does it predict insignificantly small values at long-time exposures. Our model predicts that muscle tissue cannot sustain pressure loads much longer than about 35 hours before tissue damage or death occurs.

Linder-Ganz [33] and Gefen [32] proposed a sigmoid model. But, because their model does not have an *x*-intercept, it predicts that tissue can bear a pressure load just over 50 mmHg for infinite time. This result is in disagreement with known ischemic threshold for muscle tissue, and is at variance with a report that rat muscle tissue can tolerate internal compression stress below 15 mmHg for up to five hours [33].

Allometric [34] considerations need account to appropriately compare between rat and human data. The surface factor between a rat weighing 0.3 kg and a human weighing 70 kg is 6, and 1 hour of human time is equivalent to 3.9 hours of rat time. Thus, 15 mmHg internal compression stress applied to a rat, is equivalent to 2.5 mmHg compression stress applied to a human. Moreover, 5 rat hours are equivalent to 1.3 human hours. Thus, the sigmoid pressure-time model predicts that a human can sustain a 2.5 mmHg compression stress for 1.3 hours before tissue damage occurs. This prediction is not reasonable.

Spinal cord injury veterans gain appreciable amounts of weight [35]. Our finding that P_C transmission was slowed through fat compartment suggests that weight gain may play a short-term adaptive compensatory preventive role in response to pressure loads in patients with spinal cord injury—"a cushion effect." In addition, when considered in light of findings of Sopher and colleagues [25], our finding also suggests that there is a "cut-off point" where overweight becomes harmful instead of protective. More research, however, is needed to determine whether a layer of fat, such as that found in overweight but not obese individuals, provides a protective "cushioning" effect towards prevention of pressure sores.

Our results may have important implications for interpretation of biomechanical modeling studies utilizing mathematical functions to fit pressure-time or tissue cell death-time curves [11]. All three exponential sum models tested provided reasonable parameter estimates with associated *r* values > 0.98. Thus model selection required it be made on the basis of *statistical criteria* [22, 23]. This approach increases our confidence that we chose the "correct" model from among competing models. Bone is a fourth compartment which could not be identified because of limited data resolution.

Exponential sum modeling of pressure-duration curves provides a new approach for studying the dynamics of compression *in vivo*.

FUNDING

No grants or financial aid.

CONFLICT OF INTEREST DISCLOSURE

No conflicts of interest.

REFERENCES

[1] Kohn M, Achs M, Garfinkel D. Computer simulation of metabolism in pyruvate perfused rat heart, I. Model construction. Am J Physiol 1979; 237(3): R153-R158.

[2] Bellman R, Kagiwada H, Kalaba R. Inverse problems in ecology. J Theor Biol 1966; 11: 164-67. http://dx.doi.org/10.1016/0022-5193(66)90046-4

[3] Linares O, Jacquez J, Zech L, *et al*. Norepinephrine metabolism in humans: kinetic analysis and model. J Clin Investig 1987; 80: 1332-41. http://dx.doi.org/10.1172/JCI113210

[4] Stromberg J, Linares O, Supiano M, Smith M, Foster A, Halter J. Effect of desipramine on norepinephrine metabolism in humans: interaction with aging. Am J Physiol Regul Integr Comp Physiol 1991; 261: 1484-90.

[5] Rosen S, Supiano M, Perry T, *et al*. β-Adrenergic blockade decreases norepinephrine release in humans. Am J Physiol Endocrinol Metab 1999; 258: E999-E1005.

[6] Daly A, Linares O, Smith M, Starling M, Supiano M. Dobutamine pharmacokinetics during dobutamine stress echocardiography. Am J Cardiol 1997; 79: 1381-86. http://dx.doi.org/10.1016/S0002-9149(97)00144-6

[7] Wastney M, Patterson B, Linares O, Greif P, Boston R. Investigating Biological Systems Using Modeling: Strategies and Software. San Diego: Academic Press 1999.

[8] Rust B. Fitting nature's basic functions. Part III: exponentials, sinusoids, and nonlinear least squares. Comput Sci Eng 2002; 4(4): 72-77. http://dx.doi.org/10.1109/MCISE.2002.1014982

[9] Grossman P, Linares O, Supiano M, Oral H, Mehta R, Starling M. Cardiac-specific norepinephrine mass transport and its relationship to left ventricular size and systolic performance. Am J Physiol Heart Circ Physiol 2004; 287: H878-H888. http://dx.doi.org/10.1152/ajpheart.00007.2003

[10] Cobelli C, Caumo A. Using what is accessible to measure that which is not: necessity of model of system. Metabolism 1998; 47(8): 1009-35. http://dx.doi.org/10.1016/S0026-0495(98)90360-2

[11] Gefen A. Mathematical functions and their properties as relevant to the biomechanical modeling of cell and tissue damage. J Appl Biomech 2010; 26: 93-103.

[12] Gefen A. Bioengineering Models of Deep Tissue Injury. Adv Skin Wound Care 2007; 21(1): 30-36. http://dx.doi.org/10.1097/01.ASW.0000305403.89737.6c

[13] Stefanovska A, Vodovnik L, Benko H, Turk R. Treatment of chronic wounds by means of electrical and electromagnetic fiels, Part 2. Value of FES parameters for pressure sore treatment. Med Biol Eng Comput 1993; 31: 213-20. http://dx.doi.org/10.1007/BF02458039

[14] Cukjati D, Rebersek S, Karba R, Miklavcic D. Mathematical modeling of chronic wound healing. Electro- and Magnetobiol 1998; 17(2): 237-42.

[15] Reswick J, Rogers J. Experience at Rancho Los Amigos Hospital with devices and techniques to prevent pressure ulcers. In: Kenedi R, Cowden J, Scales J, Eds. Bedsore Biomechanics. London: Macmillan Press 1976; pp. 301-310.

[16] Gefen A. Reswick and Rogers pressure-time curve for pressure ulcer risk. Part 1. Nurs Stand 2009; 23(45): 64-74.

[17] Jacob H. Using published data. Beverly Hills: Sage Publications Inc. 1984.

[18] Wastney M, Wang X, Boston R. Publishing, interpreting, and accessing models. J Franklin Inst 1998; 335B: 281-301.

[19] Boston R, Moate P. A novel minimal model to describe NEFA kinetics following an intravenous glucose challenge. Am J Physiol Regul Integr Comp Physiol 2008; 294: R1140-R1147.

[20] Boston R, Moate P. NEFA minimal model parameters estimated from the oral glucose tolerance test and the meal tolerance test. Am J Physiol Regul Integr Comp Physiol 2008; 295: R395-R403.

[21] Grief P, Wastney M, Linares O, Boston R. Balancing needs, efficiency, and functionality in the provision of modeling software: a perspective of the NIH WinSAAM Project. Adv Exp Med Biol 1998; 445: 3-20.

[22] Carson E, Cobelli C, Finkelstein L. Mathematical Modeling of Metabolic and Endocrine Systems: Model Formulation, Identification and Validation. New York: Wiley 1983.

[23] Landaw E, Distefano III J. Multiexponential, multicompartmental, and noncompartmental modeling. II. Data analysis and statistical considerations. Am J Physiol Regul Integr Comp Physiol 1984; 246: 665-77.

[24] Berman M. the formulation and testing of models. Ann New York Acad Sci 1963; 108: 182-94. http://dx.doi.org/10.1111/j.1749-6632.1963.tb13373.x

[25] Sopher R, Nixon J, Gorecki C, Gefen A. Exposure to internal muscle tissue loads under the ischial tuberosities during sitting is elevated at abnormally high or low body mass indices. J Biomech 2010; 43: 280-86. http://dx.doi.org/10.1016/j.jbiomech.2009.08.021

[26] Sun Q, Lin F, Ruberte L, Nam E, Hendrix R, Makhsous M. FE modeling and analysis of compressed human buttock-thign tissue. ISB XXth Congress Cleveland, OH 2005; 715.

[27] Landis E. Capillary pressure and capillary permeability. Physiol Rev 1934; 14: 404-81.

[28] McLennan C, McLennan M, Landis E. The effect of external pressure on the vascular volume of the forearm and its relation to capillary blood pressure and venous pressure. J Clin Investig 1942; 21: 319-38. http://dx.doi.org/10.1172/JCI101306

[29] Eichna L, Bordley J. Capillary blood pressure in man. Comparison of direct and indirect methods of measurement. J Clin Investig 1939; 18: 695-704. http://dx.doi.org/10.1172/JCI101085

[30] Eichna L, Bordley J. Capillary blood pressure in man. Direct measurements in the digits of normal and hypertensive subjects during vasoconstriction and vasofilation variously induced. J Clin Investig 1942; 21: 711-29. http://dx.doi.org/10.1172/JCI101347

[31] Tooke J, Tindall H, McNicol G. The influence of combined oral contraceptive pill and menstrual cycle phase on digital microvascular hemodynamics. Clin Sci (Lond) 1981; 61: 91-95.

[32] Gefen A. Reswick and Rogers pressure-time curve for pressure ulcer risk. Part 2. Nurs Stand 2009; 23(46): 40-44.

[33] Linder-Ganz E, Engelberg S, Scheinowitz M, Gefen A. Pressure-time cell death threshold for albino rat skeletal

muscles as related to pressure sore bimechanics. J Biomech 2006; 39(14): 2725-32.
http://dx.doi.org/10.1016/j.jbiomech.2005.08.010

[34] Ings R. Interspecies scaling and comparisons in drug development and toxicokinetics. Xenobiotica 1990; 20: 1201-31.
http://dx.doi.org/10.3109/00498259009046839

[35] Gupta N, White K, Sanford P. Body mass index in spinal chord injury: a retrospective study. Spinal Chord 2006; 44(2): 92-94.
http://dx.doi.org/10.1038/sj.sc.3101790

Received on 14-10-2012 Accepted on 12-11-2012 Published on 16-11-2012

http://dx.doi.org/10.6000/1927-5129.2012.08.02.64